Experimental and Numerical Study on Energy Efficiency of Micro-Evaporators

N. Mouline, T. El Messaoudi, J. Bouzaid*

Laboratory of Chemistry and Environment, Faculty of Sciences, Abdelmalek Essaâdi University, Tetouan, Morocco
Laboratory of Chemistry and Environment, Faculty of Sciences, Abdelmalek Essaâdi University, Tetouan, Morocco
LMPE, ENSAM, Moulay Ismail University, Meknès, Morocco

KEYWORDS: Capillary; CFD; Evaporation; Numerical simulation.

ABSTRACT

This paper presents CFD predictions for the evaporation in a microchannel for inlet mass flux in the range 10 up to 100 kg/m²s, under atmospheric pressure. The model solves the Navier-Stokes equations along with the energy conservation equation and the species transport equations; the Volume of Fluid (VOF) methodology has been utilized to capture the liquid-vapor interface using an adaptive local grid refinement technique aiming to minimize the computational cost and achieve high resolution at the liquid-gas interface region. A two dimensional microchannel of length 1000µm and hydraulic diameter of 100µm was developed in ANSYS FLUENT 13. Results were analyzed in term of the variation of volume fraction of vapor at different locations along the microchannel.

INTRODUCTION

The demand for compact and efficient thermal systems, in which the heat exchangers play an important role, has led to the development and use of several techniques to enhance the energy efficiency. The capillary evaporation process flows is of primary importance in many natural and industrial processes (automotive, aeronautic, fire suppression, painting, medical aerosol, meteorology, etc.) [1,2,3]. Although different industrial applications involving drop evaporation are already being developed, still the theoretical knowledge on the mechanisms governing the phase transition and mass/energy transports within the vapor phase is not fully understood [4].

As demonstrated previously, the mechanisms controlling two-phase velocities, pressure drops and heat transfer coefficients, at the micro-scale, are inherently related to flow regimes. Saisorn and Wongwises [5] performed experiments in a microchannel, and presented a flow pattern map. Megahed and Hassan [6] conducted an experimental investigation of the pressure drop and flow visualization of two-phase flow in a rectangular microchannel heat sink. Bubble growth and flow regimes were observed by high speed visualization, identifying three flow boiling regimes: bubbly, slug, and annular. Huh et al. [7] investigated the characteristics of flow boiling in a microchannel, such as pressure drops and temperature fluctuations in a long time period, which exactly matched the transition of two alternating flow patterns: bubbly/slug flow and elongated slug/semi-annular flow.

In addition to experimental studies, the emergence of powerful computers and robust numerical techniques in the last few decades has made the numerical solution of two phase conservation equations possible. Homogeneous Mixture Model (HEM) was developed on two-phase forced convection in microchannels by Sarangi et al. [8], consisting of continuous and differentiable correlations and one momentum equation for the entire flow. It assumes that the dispersed and the continuous phase are combined together and modeled as a new, continuous phase. However, no-slip conditions between the liquid and the vapor phase may cause the inaccurate fluid fractions and pressure drop prediction. Two Fluid Model (TFM) is taken to be one of the most widely used two phase flow model: each phase is represented by its own specific momentum, mass and energy equations. The discontinuity in flow pattern transitions becomes a primary limitation of this model. Drift Flux Model (DFX) [9] is a model with intermediate complexity, which is smooth and differentiable, yet still accounts for the slip between the fluids. But, it requires a large number of empirical parameters, and is only valuable when the drift velocity is significantly larger than the volumetric flux. In our previous study [10], HEM and TFM were established to analyze 1D microchannel flow boiling and captured the point of the boiling onset. For interface propagation in two phase flow problems, there are many choices, e.g. front tracking, phase field, volume-of-fluid (VOF), and level set method (LSM). The VOF multiphase flow model was proposed by Zhuan and Wang [11] to study nucleate boiling in microchannels and had good agreements with experimental data.
Previous CFD simulations [12-15] have mostly used the $K-\varepsilon$ turbulence model for simulations. The $K-\varepsilon$ turbulence model only provides time averaged information about the flow, and the transient behavior of the flow has not received much attention. Since LES can successfully capture the details of small-scale flow structures in flows of steam jet into water, it was thought desirable to carry out CFD simulations using this model, since it is

known to predict the transient phenomena very well for single phase [16] and bubbly two phase [17,13] flows. In the case of simulation of two-phase flows, the Volume of Fluid (VOF) method can be used to solve the advection equation of the volume fraction and accurately predict the interface. The VOF method is widely employed in numerical simulation of free surface flows, e.g. drop collision, liquid sloshing, fluid jetting, and spray deposition [18]. The VOF method is also able to treat both large deformations of an interface and small-scale interface topologies, such as breakup and reconnection. Additionally, the VOF method has the advantage of better volume-conservation than any other fixed grid interface or volume-tracking methodology [19]. Thus, the phenomena of steam injection into subcooled water can be tracked by the VOF method.

The aim of the present work, firstly motivated by the necessity to include the above described complex drop evaporation mechanisms in spray numerical simulations through relatively simple sub-models, is to propose a general CFD approach to model the evaporation from small scales. The following sections report a numerical approach that allows the experimental conditions for the steady-state evaporation rate, allows a transient two-dimensional solution of the governing equations. The local vapor/liquid flux distribution is obtained for that different boundary conditions and an exact relation with the local capillary forces is found.

NUMERICAL MODELLING

ANSYS Fluent (Release 13) is used to perform the numerical work. The volume of fluid (VOF) model is adopted to capture the liquid vapor interface in this simulation. This model accomplishes interface tracking by solving an additional continuity-like equation for the volume fraction. The two phases are assumed to be incompressible and not penetrate each other. The sum of the volume fractions of the two phases in each cell is unity. In the present work, a transit numerical method is adopted and the governing equations are given below:

Governing Equations

Continuity equation

The global continuity equation of two phase flow is given by:

$$\frac{\partial \rho}{\partial t} + \nabla(\rho \mathbf{V}) = 0 \quad (1)$$

Momentum equation

Single momentum equation is solved throughout the domain, and the resulting velocity field is shared among the phases. The momentum equation, shown below, is dependent on the volume fractions of all phases through the properties ρ and μ.

$$\frac{\partial(\rho \mathbf{V})}{\partial t} + \nabla(\rho \mathbf{V}\mathbf{V}) = -\nabla P + \nabla[\mu(\nabla \mathbf{V} + \nabla \mathbf{V}')] + \mathbf{F} \quad (2)$$

Where ρ and μ are the mixture density and viscosity defined as:

$\rho = \rho_l \alpha_l + \rho_v \alpha_v$

$\mu = \mu_l \alpha_l + \mu_v \alpha_v$

α_l and α_v are the liquid and vapor fraction respectively

Energy equation

The energy equation, also shared among the phases, is shown below.

$$\frac{\partial(\rho \mathbf{E})}{\partial t} + \nabla[\mathbf{V}(\rho E + P)] = \nabla\left(K_{eff} \nabla T\right) + S_h \quad (3)$$

S_h is the energy source term associated with the liquid-vapor phase change determined as:

$$S_h = h_{lv} S_l \quad (4)$$

The effective thermal conductivity k_{eff} is given by:

$$k_{eff} = k_l \alpha_l + k_v \alpha_v \quad (5)$$

$$\alpha_l + \alpha_v = 1 \quad (6)$$

The VOF model treats energy, E, and temperature, T, as mass averaged variables:

$$E = \frac{\sum_{q=1}^{n} \alpha_q \rho_q E_q}{\sum_{q=1}^{n} \alpha_q \rho_q} \quad (7)$$

Where E_q for each phase is based on the specific heat of that phase and the shared temperature.

Interfacial Phase Change

The mass transfer model developed by Lee [20] is employed in the present work which assumes a constant temperature (saturation temperature Ts) at the liquid vapor interface. As described in Eq. (8), when the temperature of the liquid phase is higher than the saturation temperature, the liquid phase turns into the vapor phase, and vice versa. In the case of a lower liquid temperature or a higher vapor temperature than the saturation temperature, the mass transfer through the phase interface is zero.

Liquid mass source

$$S_l = \begin{cases} f_0 \rho_v \alpha_v (T_s - T); \text{if } T < T_s \\ f_0 \rho_l \alpha_{lv} (T_s - T); \text{if } T > T_s \end{cases}$$

Vapor mass source

$$S_v = \begin{cases} -f_0 \rho_v \alpha_v (T_s - T); \text{if } T < T_s \\ -f_0 \rho_l \alpha_{lv} (T_s - T); \text{if } T > T_s \end{cases} \quad (8)$$

Where f_0 is an adjustable parameter used to reduce the temperature difference between T and Ts to negligibly small values.

Computational Domain

A computational domain with a total length of 10mm and a hydraulic diameter of 200µm is adopted in the present work for horizontal smooth square microchannel is shown in Figure 1. This particular geometry was chosen because rectangular channels with hydraulic diameters up to 1mm can be economically fabricated using wire sawing, they are extensively used in heat sinks for chip cooling. The grid used in the simulation had around 20000 cells and the time step was 10^{-3}s. A mass flow inlet condition at the microchannel inlet was specified for the liquid phase with mixture temperature of 327.15K, and a pressure-outlet boundary condition was given at the channel outlet. Different boundary conditions at channel walls were specified in each simulation keeping the other parameters same. Domain discretization was done considering a structure grid consisting of hexahedral elements. Since the flow is symmetrical, only half geometry is used, and a symmetry boundary condition is adopted on the XZ plane.

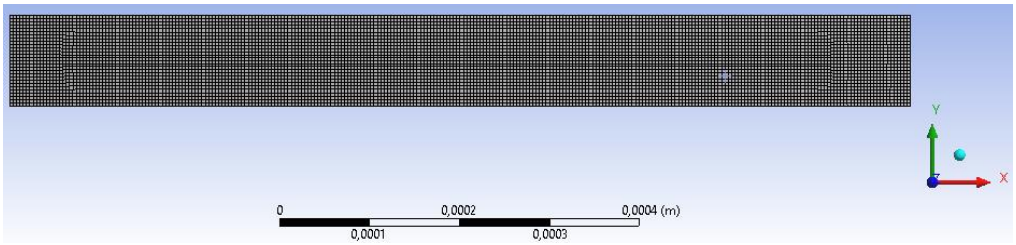

Figure 1: Computational domain

Simulation Condition

Water was used as the working fluid, whose thermophysical properties at the saturation temperature corresponding to an operating pressure 1bar were obtained from the material database of Fluent, are shown in table 1. The SIMPLE algorithm was employed for pressure-velocity coupling and the implicit scheme was used in the time discretization. The second order upwind discretization schemes were employed for energy equations and Geo-Reconstruct for the volume fraction equations, while the bounded central difference scheme was used for spatial discretization for LES.

All the solutions, except for the energy solutions, were considered to be fully converged when the sum of residuals was below $1x10^{-3}$, while for solutions of energy the sum of residuals was below $1x10^{-6}$.

Table 1. Properties of working fluids used in the simulation

Properties	***Water-liquid***	***water-vapor***
Density(kg/m^3)	1000	0.5542
Cp($J/kg.K$)	4182	2014
Thermal conductivity (W/m.K)	0.6	0.0261
Viscosity (kg/m.s)	0.009	$1.34\ 10^{-5}$
Molecular Weight(kg/kgmol)	18.015	18.0152
Reference temperature (K)	298.15	298.15

RESULTS AND DISCUSSIONS

A computational analysis on the characteristics of evaporation inside the microchannel was performed. It is important to investigate how the evaporation flow are influenced by various effects such as liquid inlet mass flux and heat transfer flux along the walls. In fact, some studies have attempted to model the physical processes occurring within the microevaporator as described in Section 1 of this study. However, these studies assumed that the fluid mixture flows straight from the inlet to the outlet of the microchannel in a manner that is consistent with a fully developed flow. As a result, the evaporate flow profiles in the microevaporator have never been properly

studied. An attempt was thus made to appropriately handle the unique flow features in the caloduc systems. It is note that many variables used in this computational analysis were determined from the experimental conditions such as inlet mass flux, diameter size, and heat flux imposed in the outer walls.

Volume fraction

Simulation has been performed by applying a constant inlet velocity ($V = 0.005m/s$) and for three walls temperatures ($T = 380, 400\ and\ 420K$) keeping other conditions unchanged. Figure 2 show the variation of liquid and vapor volume fraction.

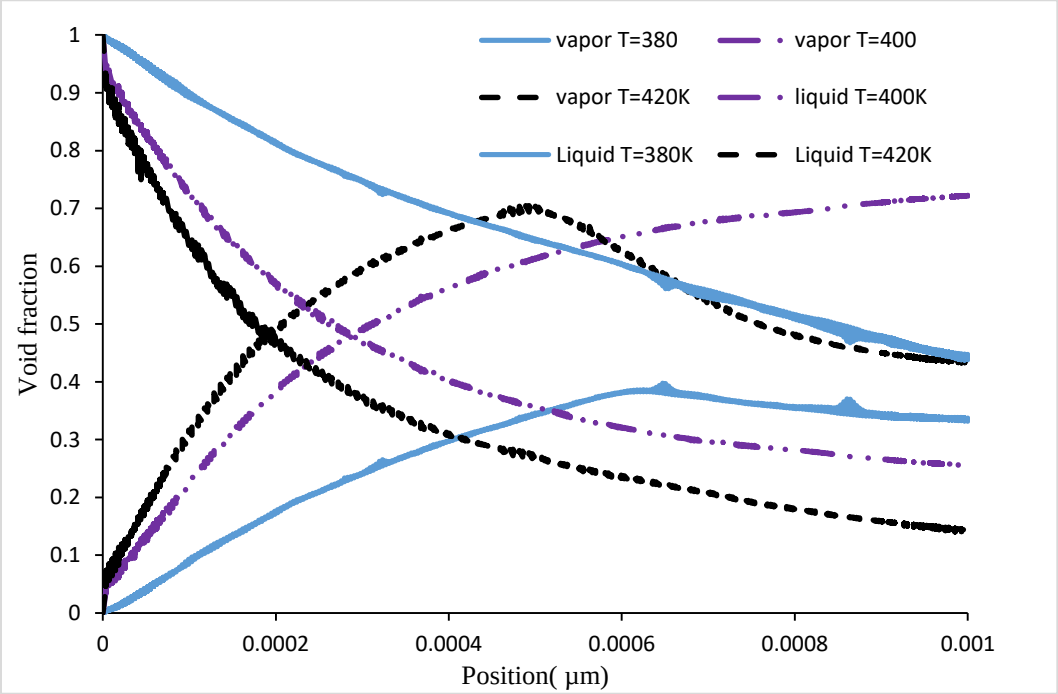

Figure 2: Variation of liquid/vapor volume fraction along the length and for different walls temperatures

As a liquid moves along the length of the microevaporator the formation of vapor increases as a result the vapor volume fraction increase along the length on the contrary to liquid phase. This finding is obvious because as the mixture in contact with the heater temperature walls. Gradual evaporation takes place within the microchannel. For a practical location the vapor volume fraction near the wall is high and it decreases towards the centerline of the microchannel. The slope of each curve near to the walls is lower which signifies high rate of vapor formation since more amount of heat is supplied near to the walls. For this reason, the variation of vapor volume fraction decreases as fluid moves along the length of the microchannel which provides sufficient time to vaporize more amount of water.

Flow structures repartitions

Although many investigators have studied the radial and axial distribution of temperature for capillary evaporation, no data have been reported about the axial and radial volume fraction and interface liquid/vapor for water evaporation.

Figure 3 displays the instantaneous evaporation rate along the microchannel. It can be seen that evaporation mainly occurs at the two-phase interface and the two-phase mixture region for steam water. It is also can be seen that evaporation rate at the liquid phase interface does not show a significant change, except in some parts of the two-phase mixture region. But for interface vapor phase change strongly and totally unstable because the capillary forces are very important inter the micro-evaporator.

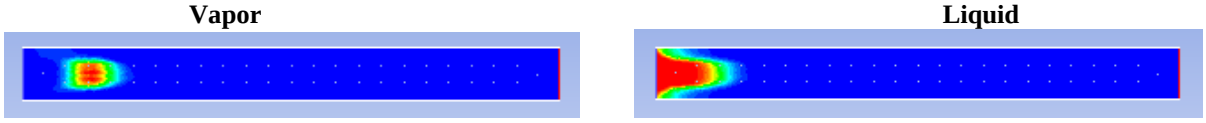

t=60s

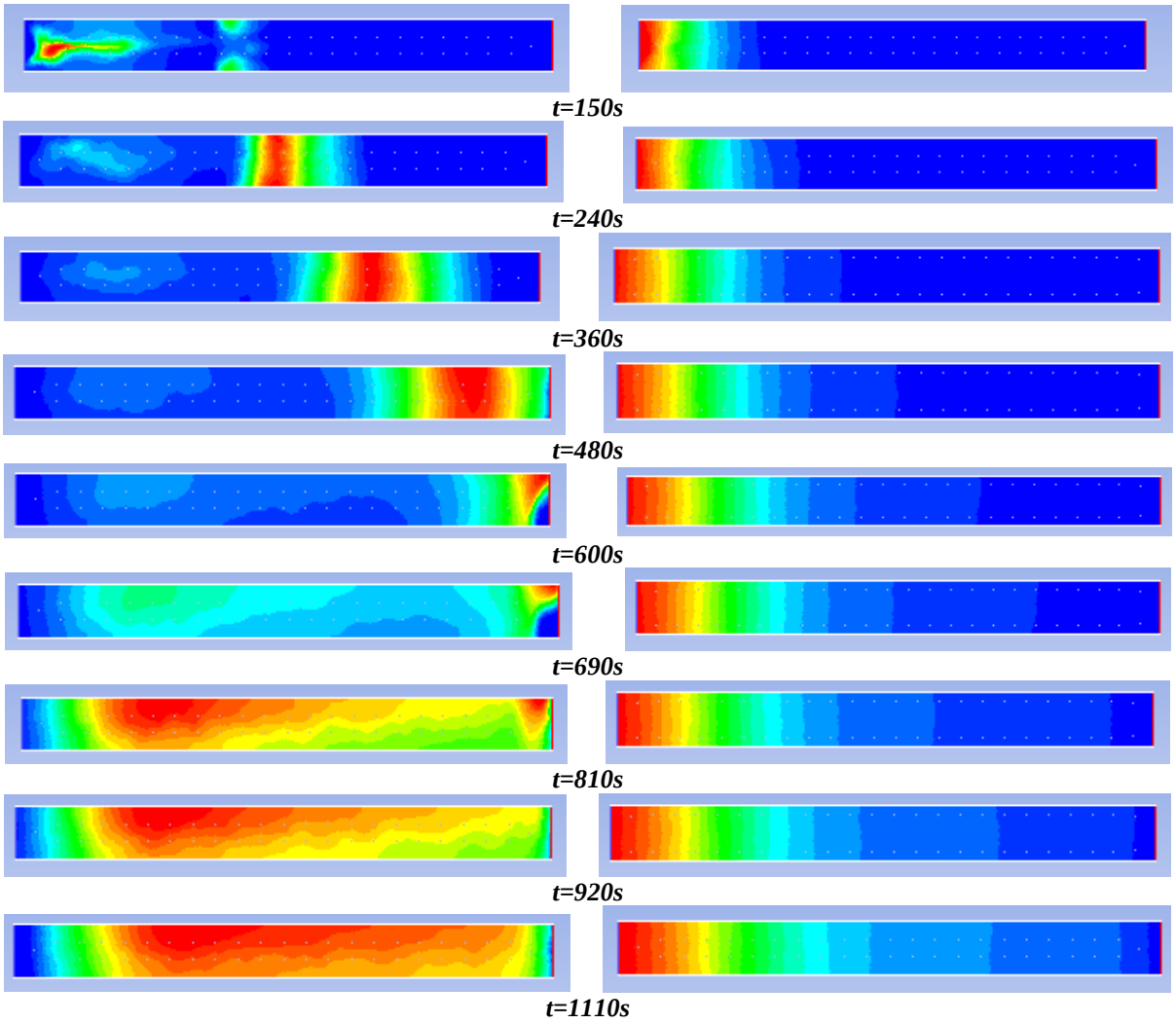

Figure 3: Temporal liquid/vapor phases repartition along the length of microchannel

CONCLUSION

CFD simulations of the evaporation in the microchannel using the VOF multiphase flow model of ANSYS Fluent 13.0 with the User Defined Function (UDF) of the energy source term have been performed.
The main conclusions can be summarized as follows:

- A good qualitative agreement was obtained with the available data reported by authors for the void fraction and the long characteristics of total evaporation.
- The centerline axial temperature increases with decreasing centerline axial velocity at the pipe inlet, which can be explained from the viewpoint of Newton's law of cooling.
- The evaporation phase change increases with increasing the wall temperature or the heat flux imposed.
- Computational process modeling using a flow package FLUENT was performed to investigate the characteristics of vapor and liquid distribution within the caloduc microevaporator area for different boundary conditions at channel walls during an evaporation heat transfer in a two-phase flow, can be extended to study the flows instabilities as well as the effects of channel geometries on vapor fraction.

REFERENCES

1. S. Tonini, G.E. Cossali, “One-dimensional analytical approach to modelling evaporation and heating of deformed drops”, International Journal of Heat and Mass Transfer, 97, 301-307, 2016.
2. V.A. Popkov, G.M. Dugacheva, V.Y. Reshetnyak, N.V. Mashnina, “Purification of praziquantel by the method of directional sublimation”, Pharm. Chem. J. 29 (6), 420–421, 1995.
3. Z. Zhifu, W. Guoxiang, C. Bin, G. Liejin, W. Yueshe, “Evaluation of evaporation models for single moving droplet with a high evaporation rate”, Powder Technol, 240, 95–102, 2013.
4. C.T. Crowe, M. Sommerfeld, Y. Tsuji, “Multiphase Flows with Droplets and Particles”, CRC Press, Boca Raton, 1998.

5. S. Saisorn, S. Wongwises, “An experimental investigation of two-phase air– water flow through a horizontal circular micro-channel”, Exp. Therm. Fluid Sci. 33,306–315, 2009.
6. A. Megahed, I. Hassan, “Two-phase pressure drop and flow visualization of FC- 72 in a silicon microchannel heat sink”, Int. J. Heat Fluid Flow 30, 1171– 1182, 2009.
7. C. Huh, J. Kim, M.H. Kim, “Flow pattern transition instability during flow boiling in a single microchannel”, Int. J. Heat Mass Transfer, 50, 1049–1060, 2007.
8. R.K. Sarangi, A. Bhattacharya, R.S. Prasher, “Numerical modeling of boiling heat transfer in microchannels”, Appl. Therm. Eng. 29,300–309, 2009.
9. C.S. Brooks, B. Ozar, T. Hibiki, M. Ishii, “Two-group drift-flux model in boiling flow”, Int. J. Heat Mass Transfer, 55, 6121–6129, 2012.
10. S. Zhou, B.G. Sammakia, “Modeling of two-phase micro-channel flow for thermal management of electronic systems”, in: Proceedings of IMECE2010, Vancouver, British Columbia, Canada, pp. 325–333, 2010.
11. R. Zhuan, W. Wang, “Simulation on nucleate boiling in micro-channel”, Int. J. Heat Mass Transfer, 53, 502–512, 2010.
12. S.S. Gulawani, S.K. Dahikar, C.S. Mathpati, J.B. Joshi, M.S. Shah, C.S. Rama Prasad, D.S. Shukla, “Analysis of flow pattern and heat transfer in direct contact condensation”, Chem. Eng. Sci. 64, 1719 -1738, 2009.
13. S.S. Gulawani, J.B. Joshi, M.S. Shah, C.S. RamaPrasad, D.S. Shukla, “CFD analysis of flow pattern and heat transfer in direct contact steam condensation”, Chem. Eng. Sci. 61, 5204 -5220, 2006.
14. A. Shah, I.R. Chughtai, M.H. Inayat, “Numerical simulation of direct-contact condensation from a supersonic steam jet in subcooled water”, Chin. J. Chem. Eng. 18, 577 -587, 2010.
15. G. Patel, V. Tanskanen, R. Kyrki-Rajamaki, “Numerical modelling of low Reynolds number direct contact condensation in a suppression pool test facility”, Ann. Nucl. Energy 71, 376 -387, 2014.
16. T. Lu, X.G. Zhu, H.T. Li, “Large-eddy simulation of thermal stratification in a straight branch of a tee junction with or without leakage”, Prog. Nucl. Energy 64, 41 -46, 2013.
17. N.G. Deen, T. Solberg, B.H. Hjertager, “Large eddy simulation of the gas-liquid flow in a square cross-sectioned bubble column”,Chem. Eng. Sci. 56, 6341 -6349, 2001.
18. T. Sriveerakul, S. Aphornratana, K. Chunnanond, “Performance prediction of steam ejector using computational fluid dynamics: part 1. Validation of the CFD results”, Int. J. Therm. Sci. 46, 812 -822, 2007.
19. D. Munoz-Esparza, J.M. Buchlin, K. Myrillas, R. Berger, “Numerical investigation of impinging gas jets onto deformable liquid layers”, Appl. Math Modell. 36, 2687 -2700, 2012.
20. W.H. Lee, “A Pressure Iteration Scheme for Two-phase Flow Modeling”. Washington, DC: Hemisphere, 1980.